

## Chapter 9

# Non-Linear Time-Frequency Distributions

In Chapters 7 and 8 two time-frequency distributions were discussed: the spectrogram and the scalogram. Both distributions are the result of linear filtering and subsequent forming of the squared magnitude. In this chapter time-frequency distributions derived in a different manner will be considered. Contrary to spectrograms and scalograms, their resolution is not restricted by the uncertainty principle. Although these methods do not yield positive distributions in all cases, they allow extremely good insight into signal properties within certain applications.

### 9.1 The Ambiguity Function

The goal of the following considerations is to describe the relationship between signals and their time as well as frequency-shifted versions. We start by looking at time and frequency shifts separately.

**Time-Shifted Signals.** The distance  $d(\mathbf{x}, \mathbf{x}_\tau)$  between an energy signal  $\mathbf{x}(t)$  and its time-shifted version  $\mathbf{x}_\tau(t) = \mathbf{x}(t + \tau)$  is related to the autocorrelation function  $r_{\mathbf{x}\mathbf{x}}^E(\tau)$ . Here the following holds (cf. (1.38)):

$$d(\mathbf{x}_\tau, \mathbf{x})^2 = 2 \|\mathbf{x}\|^2 - 2 \Re\{r_{\mathbf{x}\mathbf{x}}^E(\tau)\}, \quad (9.1)$$

where

$$r_{xx}^E(\tau) = \langle \mathbf{x}_\tau, \mathbf{x} \rangle = \int_{-\infty}^{\infty} x^*(t) x(t + \tau) dt. \quad (9.2)$$

As explained in Section 1.2,  $r_{xx}^E(\tau)$  can also be understood as the inverse Fourier transform of the energy density spectrum  $S_{xx}^E(\omega) = |X(\omega)|^2$ :

$$\begin{aligned} r_{xx}^E(\tau) &= \frac{1}{2\pi} \int_{-\infty}^{\infty} S_{xx}^E(\omega) e^{j\omega\tau} d\omega \\ &= \frac{1}{2\pi} \int_{-\infty}^{\infty} X^*(\omega) X(\omega) e^{j\omega\tau} d\omega. \end{aligned} \quad (9.3)$$

In applications in which the signal  $x(t)$  is transmitted and the time shift  $\tau$  is to be estimated from the received signal  $x(t + \tau)$ , it is important that  $x(t)$  and  $x(t + \tau)$  are as dissimilar as possible for  $\tau \neq 0$ . That is, the transmitted signal  $x(t)$  should have an autocorrelation function that is as Dirac-shaped as possible. In the frequency domain this means that the energy density spectrum should be as constant as possible.

**Frequency-Shifted Signals.** Frequency-shifted versions of a signal  $x(t)$  are often produced due to the Doppler effect. If one wants to estimate such frequency shifts in order to determine the velocity of a moving object, the distance between a signal  $x(t)$  and its frequency-shifted version  $x_\nu(t) = x(t)e^{j\nu t}$  is of crucial importance. The distance is given by

$$d(\mathbf{x}, \mathbf{x}_\nu) = 2 \|\mathbf{x}\|^2 - 2 \Re\{\langle \mathbf{x}_\nu, \mathbf{x} \rangle\}. \quad (9.4)$$

For the inner product  $\langle \mathbf{x}_\nu, \mathbf{x} \rangle$  in (9.4) we will henceforth use the abbreviation  $\rho_{xx}^E(\nu)$ . We have

$$\begin{aligned} \rho_{xx}^E(\nu) &= \langle \mathbf{x}_\nu, \mathbf{x} \rangle \\ &= \int_{-\infty}^{\infty} x^*(t) x(t) e^{j\nu t} dt \\ &= \int_{-\infty}^{\infty} s_{xx}^E(t) e^{j\nu t} dt \quad \text{with} \quad s_{xx}^E(t) = |x(t)|^2, \end{aligned} \quad (9.5)$$

where  $s_{xx}^E(t)$  can be viewed as the temporal energy density.<sup>1</sup> Comparing (9.5) with (9.3) shows a certain resemblance of the formulae for  $r_{xx}^E(\tau)$  and  $\rho_{xx}^E(\nu)$ ,

<sup>1</sup>In (9.5) we have an inverse Fourier transform in which the usual prefactor  $1/2\pi$  does not occur because we integrate over  $t$ , not over  $\omega$ . This peculiarity could be avoided if  $\nu$  was replaced by  $-\nu$  and (9.5) was interpreted as a forward Fourier transform. However, this would lead to other inconveniences in the remainder of this chapter.

however, with the time frequency domains being exchanged. This becomes even more obvious if  $\rho_{xx}^E(\nu)$  is stated in the frequency domain:

$$\rho_{xx}^E(\nu) = \frac{1}{2\pi} \int_{-\infty}^{\infty} X(\omega) X^*(\omega + \nu) d\omega. \quad (9.6)$$

We see that  $\rho_{xx}^E(\nu)$  can be seen as the autocorrelation function of  $X(\omega)$ .

**Time and Frequency-Shifted Signals.** Let us consider the signals

$$\begin{aligned} \mathbf{x}_{-\frac{\tau}{2}, -\frac{\nu}{2}}(t) &= \mathbf{x}\left(t - \frac{\tau}{2}\right) e^{-j\nu t/2}, \\ \mathbf{x}_{\frac{\tau}{2}, \frac{\nu}{2}} &= \mathbf{x}\left(t + \frac{\tau}{2}\right) e^{j\nu t/2}, \end{aligned} \quad (9.7)$$

which are time and frequency shifted versions of one another, centered around  $x(t)$ . With the abbreviation

$$A_{xx}(\nu, \tau) = \langle \mathbf{x}_{\frac{\tau}{2}, \frac{\nu}{2}}, \mathbf{x}_{-\frac{\tau}{2}, -\frac{\nu}{2}} \rangle \quad (9.8)$$

for the so-called *time-frequency autocorrelation function* or *ambiguity function*<sup>2</sup> we get

$$\begin{aligned} d(\mathbf{x}_{-\frac{\tau}{2}, -\frac{\nu}{2}}, \mathbf{x}_{\frac{\tau}{2}, \frac{\nu}{2}}) &= 2 \|\mathbf{x}\|^2 - 2 \Re\{\langle \mathbf{x}_{\frac{\tau}{2}, \frac{\nu}{2}}, \mathbf{x}_{-\frac{\tau}{2}, -\frac{\nu}{2}} \rangle\} \\ &= 2 \|\mathbf{x}\|^2 - 2 \Re\{A_{xx}(\nu, \tau)\}. \end{aligned} \quad (9.9)$$

Thus, the real part of  $A_{xx}(\nu, \tau)$  is related to the distance between both signals.

In non-abbreviated form (9.8) is

$$A_{xx}(\nu, \tau) = \int_{-\infty}^{\infty} \mathbf{x}^*\left(t - \frac{\tau}{2}\right) \mathbf{x}\left(t + \frac{\tau}{2}\right) e^{j\nu t} dt. \quad (9.10)$$

Via Parseval's relation we obtain an expression for computing  $A_{xx}(\nu, \tau)$  in the frequency domain

$$A_{xx}(\nu, \tau) = \frac{1}{2\pi} \int_{-\infty}^{\infty} X\left(\omega - \frac{\nu}{2}\right) X^*\left(\omega + \frac{\nu}{2}\right) e^{j\omega\tau} d\omega. \quad (9.11)$$

<sup>2</sup>We find different definitions of this term in the literature. Some authors also use it for the term  $|A_{xx}(\nu, \tau)|^2$  [150].

**Example.** We consider the Gaussian signal

$$x(t) = \left(\frac{\alpha}{\pi}\right)^{\frac{1}{4}} e^{-\frac{1}{2}\alpha t^2}, \quad (9.12)$$

which satisfies  $\|x\| = 1$ . Using the correspondence

$$e^{-\pi t^2} \longleftrightarrow e^{-\frac{1}{4\pi^2}\omega^2}, \quad (9.13)$$

we obtain

$$A_{xx}(\nu, \tau) = e^{-\frac{\alpha}{4}\tau^2} e^{-\frac{1}{4\alpha}\nu^2}. \quad (9.14)$$

Thus, the ambiguity function is a two-dimensional Gaussian function whose center is located at the origin of the  $\tau$ - $\nu$  plane.

### Properties of the Ambiguity Function.

1. A time shift of the input signal leads to a modulation of the ambiguity function with respect to the frequency shift  $\nu$ :

$$\tilde{x}(t) = x(t - t_0) \quad \Rightarrow \quad A_{\tilde{x}\tilde{x}}(\nu, \tau) = e^{j\nu t_0} A_{xx}(\nu, \tau). \quad (9.15)$$

This relation can easily be derived from (9.11) by exploiting the fact that  $\tilde{X}(\omega) = e^{-j\omega t_0} X(\omega)$ .

2. A modulation of the input signal leads to a modulation of the ambiguity function with respect to  $\tau$ :

$$\tilde{x}(t) = e^{j\omega_0 t} x(t) \quad \Rightarrow \quad A_{\tilde{x}\tilde{x}}(\nu, \tau) = e^{j\omega_0 \tau} A_{xx}(\nu, \tau). \quad (9.16)$$

This is directly derived from (9.10).

3. The ambiguity function has its maximum at the origin,

$$\max\{A_{xx}(\nu, \tau)\} = A_{xx}(0, 0) = E_x, \quad (9.17)$$

where  $E_x$  is the signal energy. A modulation and/or time shift of the signal  $x(t)$  leads to a modulation of the ambiguity function, but the principal position in the  $\tau$ - $\nu$  plane is not affected.

**Radar Uncertainty Principle.** The classical problem in radar is to find signals  $x(t)$  that allow estimation of time and frequency shifts with high precision. Therefore, when designing an appropriate signal  $x(t)$  the expression

$$|A_{xx}(\nu, \tau)|^2$$

is considered, which contains information on the possible resolution of a given  $x(t)$  in the  $\tau$ - $\nu$  plane. The ideal of having an impulse located at the origin of the  $\tau$ - $\nu$  plane cannot be realized since we have [150]

$$\frac{1}{2\pi} \int_{-\infty}^{\infty} \int_{-\infty}^{\infty} |A_{xx}(\nu, \tau)|^2 d\tau d\nu = |A_{xx}(0, 0)|^2 = E_x^2. \quad (9.18)$$

That is, if we achieve that  $|A_{xx}(\nu, \tau)|^2$  takes on the form of an impulse at the origin, it necessarily has to grow in other regions of the  $\tau$ - $\nu$  plane because of the limited maximal value  $|A_{xx}(0, 0)|^2 = E_x^2$ . For this reason, (9.18) is also referred to as the *radar uncertainty principle*.

**Cross Ambiguity Function.** Finally we want to remark that, analogous to the cross correlation, so-called *cross ambiguity functions* are defined:

$$\begin{aligned} A_{yx}(\nu, \tau) &= \int_{-\infty}^{\infty} x(t + \frac{\tau}{2}) y^*(t - \frac{\tau}{2}) e^{j\nu t} dt \\ &= \frac{1}{2\pi} \int_{-\infty}^{\infty} X(\omega - \frac{\nu}{2}) Y^*(\omega + \frac{\nu}{2}) e^{j\omega\tau} d\omega. \end{aligned} \quad (9.19)$$

## 9.2 The Wigner Distribution

### 9.2.1 Definition and Properties

The Wigner distribution is a tool for time-frequency analysis, which has gained more and more importance owing to many extraordinary characteristics. In order to highlight the motivation for the definition of the Wigner distribution, we first look at the ambiguity function. From  $A_{xx}(\nu, \tau)$  we obtain for  $\nu = 0$  the temporal autocorrelation function

$$r_{xx}^E(\tau) = A_{xx}(0, \tau), \quad (9.20)$$

from which we derive the energy density spectrum by means of the Fourier transform:

$$\begin{aligned} S_{xx}^E(\omega) &= \int_{-\infty}^{\infty} r_{xx}^E(\tau) e^{-j\omega\tau} d\tau \\ &= \int_{-\infty}^{\infty} A_{xx}(0, \tau) e^{-j\omega\tau} d\tau. \end{aligned} \quad (9.21)$$

On the other hand, we get the autocorrelation function  $\rho_{xx}^E(\nu)$  of the spectrum  $X(\omega)$  from  $A_{xx}(\nu, \tau)$  for  $\tau = 0$ :

$$\rho_{xx}^E(\nu) = A_{xx}(\nu, 0). \quad (9.22)$$

The temporal energy density  $s_{xx}^E(t)$  is the Fourier transform of  $\rho_{xx}^E(\nu)$ :

$$\begin{aligned} s_{xx}^E(t) &= \frac{1}{2\pi} \int_{-\infty}^{\infty} \rho_{xx}^E(\nu) e^{-j\nu t} d\nu \\ &= \frac{1}{2\pi} \int_{-\infty}^{\infty} A_{xx}(\nu, 0) e^{-j\nu t} d\nu. \end{aligned} \quad (9.23)$$

These relationships suggest defining a two-dimensional *time-frequency distribution*  $W_{xx}(t, \omega)$  as the two-dimensional Fourier transform of  $A_{xx}(\nu, \tau)$ :

$$W_{xx}(t, \omega) = \frac{1}{2\pi} \int_{-\infty}^{\infty} \int_{-\infty}^{\infty} A_{xx}(\nu, \tau) e^{-j\nu t} e^{-j\omega \tau} d\nu d\tau. \quad (9.24)$$

The time-frequency distribution  $W_{xx}(t, \omega)$  is known as the *Wigner distribution*.<sup>3</sup>

The two-dimensional Fourier transform in (9.24) can also be viewed as performing two subsequent one-dimensional Fourier transforms with respect to  $\tau$  and  $\nu$ . The transform with respect to  $\nu$  yields the *temporal autocorrelation function*<sup>4</sup>

$$\begin{aligned} \phi_{xx}(t, \tau) &= \frac{1}{2\pi} \int_{-\infty}^{\infty} A_{xx}(\nu, \tau) e^{-j\nu t} d\nu \\ &= x^*(t - \frac{\tau}{2}) x(t + \frac{\tau}{2}). \end{aligned} \quad (9.25)$$

The Fourier transform of  $A_{xx}(\nu, \tau)$  with respect to  $\tau$  yields

$$\begin{aligned} \Phi_{xx}(\nu, \omega) &= \int_{-\infty}^{\infty} A_{xx}(\nu, \tau) e^{-j\omega \tau} d\tau \\ &= X(\omega - \frac{\nu}{2}) X^*(\omega + \frac{\nu}{2}). \end{aligned} \quad (9.26)$$

<sup>3</sup>Wigner used  $W_{xx}(t, \omega)$  for describing phenomena of quantum mechanics [163], Ville introduced it for signal analysis later [156], so that one also speaks of the Wigner-Ville distribution.

<sup>4</sup>If  $x(t)$  was assumed to be a random process,  $E\{\phi_{xx}(t, \tau)\}$  would be the autocorrelation function of the process.

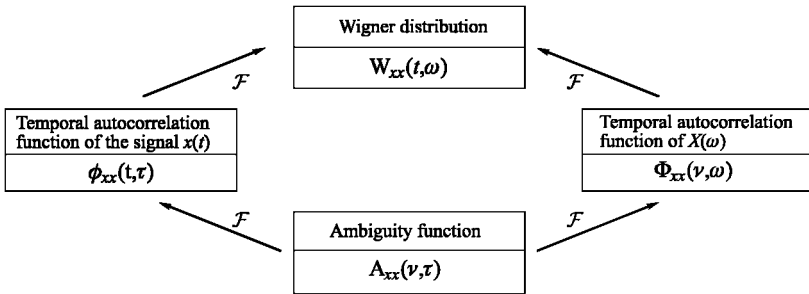


Figure 9.1. Relationship between ambiguity function and Wigner distribution.

The function  $\Phi_{xx}(\nu, \omega)$  is so to say the *temporal autocorrelation function* of  $X(\omega)$ . Altogether we obtain

$$\begin{aligned}
 W_{xx}(t, \omega) &= \int_{-\infty}^{\infty} \phi_{xx}(t, \tau) e^{-j\omega\tau} d\tau \\
 &= \frac{1}{2\pi} \int_{-\infty}^{\infty} \Phi_{xx}(\nu, \omega) e^{-j\nu t} d\nu
 \end{aligned}
 \tag{9.27}$$

with  $\phi_{xx}(t, \tau)$  according to (9.25) and  $\Phi_{xx}(\nu, \omega)$  according to (9.26), in full:

$$\begin{aligned}
 W_{xx}(t, \omega) &= \int_{-\infty}^{\infty} x^*(t - \frac{\tau}{2}) x(t + \frac{\tau}{2}) e^{-j\omega\tau} d\tau \\
 &= \frac{1}{2\pi} \int_{-\infty}^{\infty} X(\omega - \frac{\nu}{2}) X^*(\omega + \frac{\nu}{2}) e^{-j\nu t} d\nu.
 \end{aligned}
 \tag{9.28}$$

Figure 9.1 pictures the relationships mentioned above.

We speak of  $W_{xx}(t, \omega)$  as a distribution because it is supposed to reflect the distribution of the signal energy in the time-frequency plane. However, the Wigner distribution cannot be interpreted pointwise as a distribution of energy because it can also take on negative values. Apart from this restriction it has all the properties one would wish of a time-frequency distribution. The most important of these properties will be briefly listed. Since the proofs can be directly inferred from equation (9.28) by exploiting the characteristics of the Fourier transform, they are omitted.

**Some Properties of the Wigner Distribution:**

1. The Wigner distribution of an arbitrary signal  $x(t)$  is always real,

$$W_{xx}(t, \omega) = W_{xx}^*(t, \omega) = \Re\{W_{xx}(t, \omega)\}. \quad (9.29)$$

If  $x(t)$  is real itself, we conclude from (9.28), by observing the properties of the Fourier transform, that  $W_{xx}(t, \omega)$  is an even function of  $\omega$ , that is  $W_{xx}(t, \omega) = W_{xx}(t, -\omega)$ .

2. By integrating over  $\omega$  we obtain the temporal energy density

$$s_{xx}^E(t) = \frac{1}{2\pi} \int_{-\infty}^{\infty} W_{xx}(t, \omega) d\omega = |x(t)|^2. \quad (9.30)$$

3. By integrating over  $t$  we obtain the energy density spectrum

$$S_{xx}^E(\omega) = \int_{-\infty}^{\infty} W_{xx}(t, \omega) dt = |X(\omega)|^2. \quad (9.31)$$

4. Integrating over time and frequency yields the signal energy:

$$\frac{1}{2\pi} \int_{-\infty}^{\infty} \int_{-\infty}^{\infty} W_{xx}(t, \omega) d\omega dt = \int_{-\infty}^{\infty} |x(t)|^2 dt = E_x. \quad (9.32)$$

5. If a signal  $x(t)$  is non-zero in only a certain time interval, then the Wigner distribution is also restricted to this time interval:

$$\begin{aligned} x(t) &= 0 \text{ for } t < t_1 \text{ and/or } t > t_2 \\ &\Downarrow \\ W_{xx}(t, \omega) &= 0 \text{ for } t < t_1 \text{ and/or } t > t_2. \end{aligned} \quad (9.33)$$

This property immediately follows from (9.28).

6. If  $X(\omega)$  is non-zero only in a certain frequency region, then the Wigner distribution is also restricted to this frequency region:

$$\begin{aligned} X(\omega) &= 0 \text{ for } \omega < \omega_1 \text{ and/or } \omega > \omega_2 \\ &\Downarrow \\ W_{xx}(t, \omega) &= 0 \text{ for } \omega < \omega_1 \text{ and/or } \omega > \omega_2. \end{aligned} \quad (9.34)$$

7. A time shift of the signal leads to a time shift of the Wigner distribution (cf. (9.25) and (9.27)):

$$\tilde{x}(t) = x(t - t_0) \quad \Rightarrow \quad W_{\tilde{x}\tilde{x}}(t, \omega) = W_{xx}(t - t_0, \omega). \quad (9.35)$$

8. A modulation of the signal leads to a frequency shift of the Wigner distribution (cf. (9.26) and (9.27)):

$$\tilde{x}(t) = x(t)e^{j\omega_0 t} \quad \Rightarrow \quad W_{\tilde{x}\tilde{x}}(t, \omega) = W_{xx}(t, \omega - \omega_0). \quad (9.36)$$

9. A simultaneous time shift and modulation lead to a time and frequency shift of the Wigner distribution:

$$\tilde{x}(t) = x(t - t_0)e^{j\omega_0 t} \quad \Rightarrow \quad W_{\tilde{x}\tilde{x}}(t, \omega) = W_{xx}(t - t_0, \omega - \omega_0). \quad (9.37)$$

10. Time scaling leads to

$$\tilde{x}(t) = x(at) \quad \Rightarrow \quad W_{\tilde{x}\tilde{x}}(t, \omega) = \frac{1}{|a|} W_{xx}(at, \frac{\omega}{a}). \quad (9.38)$$

**Signal Reconstruction.** By an inverse Fourier transform of  $W_{xx}(t, \omega)$  with respect to  $\omega$  we obtain the function

$$\phi_{xx}(t, \tau) = x^*(t - \frac{\tau}{2}) x(t + \frac{\tau}{2}), \quad (9.39)$$

cf. (9.27). Along the line  $t = \tau/2$  we get

$$\hat{x}(\tau) = \phi_{xx}(\frac{\tau}{2}, \tau) = x^*(0) x(\tau). \quad (9.40)$$

This means that any  $x(t)$  can be perfectly reconstructed from its Wigner distribution except for the prefactor  $x^*(0)$ .

Similarly, we obtain for the spectrum

$$\hat{X}^*(\nu) = \Phi_{xx}(\frac{\nu}{2}, \nu) = X(0) X^*(\nu). \quad (9.41)$$

**Moyal's Formula for Auto-Wigner Distributions.** The squared magnitude of the inner product of two signals  $x(t)$  and  $y(t)$  is given by the inner product of their Wigner distributions [107], [18]:

$$\left| \int_{-\infty}^{\infty} x(t) y^*(t) dt \right|^2 = \frac{1}{2\pi} \iint W_{xx}(t, \omega) W_{yy}(t, \omega) dt d\omega. \quad (9.42)$$

## 9.2.2 Examples

**Signals with Linear Time-Frequency Dependency.** The prime example for demonstrating the excellent properties of the Wigner distribution in time-frequency analysis is the so-called chirp signal, a frequency modulated (FM) signal whose instantaneous frequency linearly changes with time:

$$x(t) = A e^{j\frac{1}{2}\beta t^2} e^{j\omega_0 t}. \quad (9.43)$$

We obtain

$$W_{xx}(t, \omega) = 2\pi |A|^2 \delta(\omega - \omega_0 - \beta t). \quad (9.44)$$

This means that the Wigner distribution of a linearly modulated FM signal shows the exact instantaneous frequency.

**Gaussian Signal.** We consider the signal

$$\tilde{x}(t) = e^{j\omega_0 t} x(t - t_0) \quad (9.45)$$

with

$$x(t) = \left(\frac{\alpha}{\pi}\right)^{\frac{1}{4}} e^{-\frac{1}{2}\alpha t^2}. \quad (9.46)$$

The Wigner distribution  $W_{xx}(t, \omega)$  is

$$W_{xx}(t, \omega) = 2 e^{-\alpha t^2} e^{-\frac{1}{\alpha} \omega^2}, \quad (9.47)$$

and for  $W_{\tilde{x}\tilde{x}}(t, \omega)$  we get

$$W_{\tilde{x}\tilde{x}}(t, \omega) = 2 e^{-\alpha(t - t_0)^2} e^{-\frac{1}{\alpha} [\omega - \omega_0]^2}. \quad (9.48)$$

Hence the Wigner distribution of a modulated Gaussian signal is a two-dimensional Gaussian whose center is located at  $[t_0, \omega_0]$  whereas the ambiguity function is a modulated two-dimensional Gaussian signal whose center is located at the origin of the  $\tau$ - $\nu$  plane (cf. (9.14), (9.15) and (9.16)).

**Signals with Positive Wigner Distribution.** Only signals of the form

$$x(t) = \left(\frac{\alpha}{\pi}\right)^{\frac{1}{4}} e^{-\frac{1}{2}\alpha t^2} e^{j\frac{1}{2}\beta t^2} e^{j\omega_0 t} \quad (9.49)$$

have a positive Wigner distribution [30]. The Gaussian signal and the chirp are to be regarded as special cases.

For the Wigner distribution of  $x(t)$  according to (9.49) we get

$$W_{xx}(t, \omega) = 2 e^{-\alpha t^2} e^{-\frac{1}{\alpha} [\omega - \omega_0 - \beta t]^2} \quad (9.50)$$

with  $W_{xx}(t, \omega) \geq 0 \forall t, \omega$ .

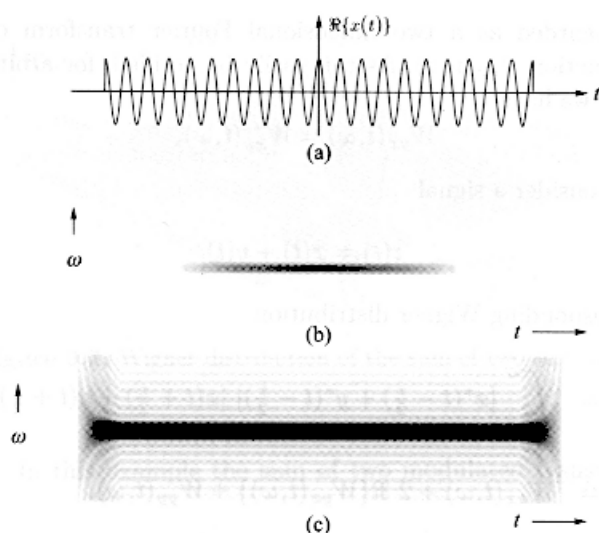


**Figure 9.2.** Time-limited exponential; (a) time signal; (b) Wigner distribution; (c) spectrogram.

**Time-Limited Exponential.** We consider an exponential limited to the interval  $[-T, T]$ :

$$x(t) = \begin{cases} e^{j\omega_0 t} & \text{for } |t| < T, \\ 0 & \text{otherwise.} \end{cases} \quad (9.51)$$

The Wigner distribution is

$$W_{xx}(t, \omega) = \begin{cases} \frac{2}{\omega - \omega_0} \sin(2(\omega - \omega_0)(T - |t|)) & \text{for } |t| < T, \\ 0 & \text{otherwise.} \end{cases} \quad (9.52)$$

Figure 9.2 shows an example of such an  $x(t)$  and two gray-scale images picturing the Wigner distribution and the spectrogram. We observe that the spectrogram is not limited to  $[-T, T]$ . Furthermore, we notice clear differences in the interference geometries of the Wigner distribution and the spectrogram.

### 9.2.3 Cross-Terms and Cross Wigner Distributions

The *cross Wigner distribution* is defined as

$$\begin{aligned} W_{yx}(t, \omega) &= \int_{-\infty}^{\infty} y^*(t - \frac{\tau}{2}) x(t + \frac{\tau}{2}) e^{-j\omega\tau} d\tau \\ &= \frac{1}{2\pi} \int_{-\infty}^{\infty} X(\omega - \frac{\nu}{2}) Y^*(\omega + \frac{\nu}{2}) e^{-j\nu t} d\nu. \end{aligned} \quad (9.53)$$

It can be regarded as a two-dimensional Fourier transform of the cross ambiguity function  $A_{yx}(\nu, \tau)$ . As can easily be verified, for arbitrary signals  $x(t)$  and  $y(t)$  we have

$$W_{yx}(t, \omega) = W_{xy}^*(t, \omega). \quad (9.54)$$

We now consider a signal

$$z(t) = x(t) + y(t) \quad (9.55)$$

and the corresponding Wigner distribution

$$\begin{aligned} W_{zz}(t, \omega) &= \int_{-\infty}^{\infty} [x^*(t - \frac{\tau}{2}) + y^*(t - \frac{\tau}{2})] [x(t + \frac{\tau}{2}) + y(t + \frac{\tau}{2})] e^{-j\omega\tau} d\tau \\ &= W_{xx}(t, \omega) + 2 \Re\{W_{yx}(t, \omega)\} + W_{yy}(t, \omega). \end{aligned} \quad (9.56)$$

We see that the Wigner distribution of the sum of two signals does not equal the sum of their respective Wigner distributions. The occurrence of cross-terms  $W_{yx}(t, \omega)$  complicates the interpretation of the Wigner distribution of real-world signals. Size and location of the interference terms are discussed in the following examples.

**Moyal's Formula for Cross Wigner Distributions.** For the inner product of two cross Wigner distributions we have [18]

$$\frac{1}{2\pi} \iint W_{x_1 y_1}(t, \omega) W_{x_2 y_2}(t, \omega) dt d\omega = \langle \mathbf{x}_1, \mathbf{y}_1 \rangle \langle \mathbf{x}_2, \mathbf{y}_2 \rangle \quad (9.57)$$

with  $\langle \mathbf{x}, \mathbf{y} \rangle = \int x(t) y^*(t) dt$ .

**Example.** We consider the sum of two complex exponentials

$$z(t) = \frac{A_1}{\sqrt{2\pi}} e^{j\omega_1 t} + \frac{A_2}{\sqrt{2\pi}} e^{j\omega_2 t}. \quad (9.58)$$

For  $W_{zz}(t, \omega)$  we get

$$\begin{aligned} W_{zz}(t, \omega) &= A_1^2 \delta(\omega - \omega_1) + A_2^2 \delta(\omega - \omega_2) \\ &\quad + 2A_1 A_2 \cos((\omega_2 - \omega_1)t) \delta(\omega - \frac{1}{2}(\omega_1 + \omega_2)) \end{aligned} \quad (9.59)$$

Figure 9.3 shows  $W_{zz}(t, \omega)$  and illustrates the influence of the cross-term  $2A_1 A_2 \cos((\omega_2 - \omega_1)t) \delta(\omega - \frac{1}{2}(\omega_1 + \omega_2))$ .

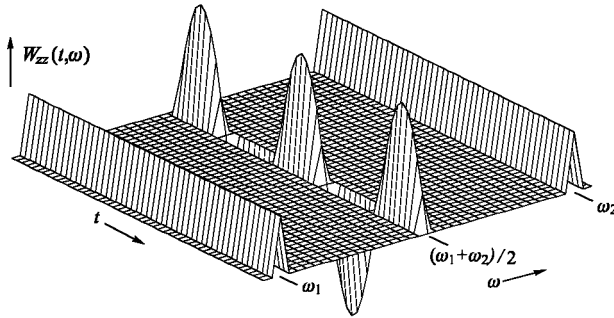


**Figure 9.3.** Wigner distribution of the sum of two sine waves.

**Example.** In this example the sum of two modulated Gaussian signals is considered:

$$z(t) = x(t) + y(t) \quad (9.60)$$

with

$$x(t) = e^{j\omega_1(t-t_1)} e^{-\frac{1}{2}\alpha(t-t_1)^2} \quad (9.61)$$

and

$$y(t) = e^{j\omega_2(t-t_2)} e^{-\frac{1}{2}\alpha(t-t_2)^2}. \quad (9.62)$$

Figures 9.4 and 9.5 show examples of the Wigner distribution. We see that the interference term lies between the two signal terms, and the modulation of the interference term takes place orthogonal to the line connecting the two signal terms. This is different for the ambiguity function, also shown in Figure 9.5. The center of the signal term is located at the origin, which results from the fact that the ambiguity function is a time-frequency autocorrelation function. The interference terms concentrate around

$$\begin{aligned} \tau_1 &= t_1 - (t_1 + t_2)/2, \\ \nu_1 &= \omega_2 - (\omega_1 + \omega_2)/2, \\ \tau_2 &= t_2 - (t_1 + t_2)/2, \\ \nu_2 &= \omega_1 - (\omega_1 + \omega_2)/2. \end{aligned}$$

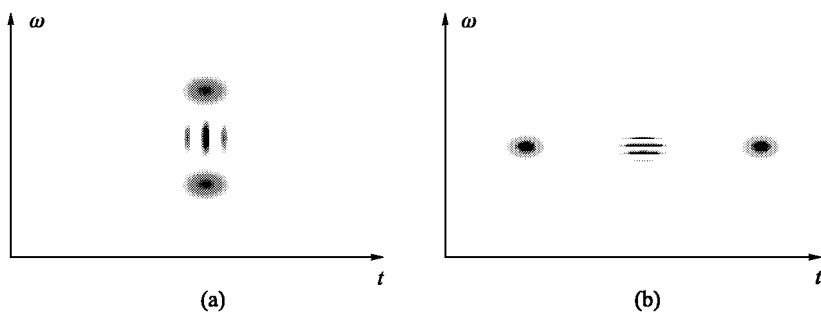


**Figure 9.4.** Wigner distribution of the sum of two modulated and time-shifted Gaussians; (a)  $t_1 = t_2, \omega_1 \neq \omega_2$ ; (b)  $t_1 \neq t_2, \omega_1 = \omega_2$ .

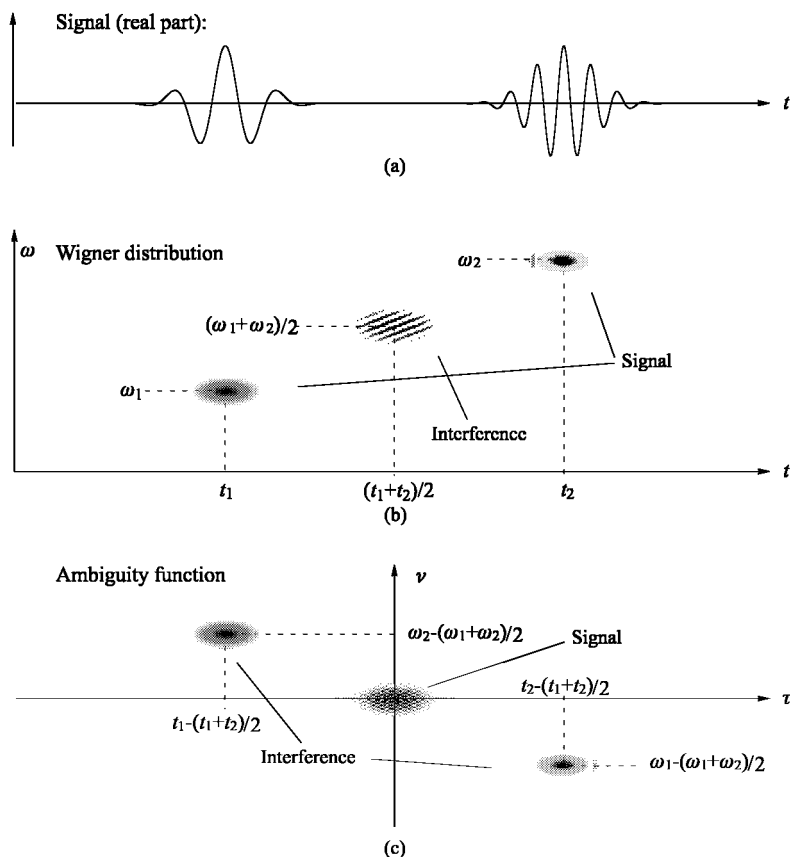


**Figure 9.5.** Wigner distribution and ambiguity function of the sum of two modulated and time-shifted Gaussians ( $t_1 \neq t_2, \omega_1 \neq \omega_2$ ).

### 9.2.4 Linear Operations

**Multiplication in the Time Domain.** We consider the signal

$$\tilde{x}(t) = x(t) h(t). \quad (9.63)$$

For the Wigner distribution we get

$$\begin{aligned} W_{\tilde{x}\tilde{x}}(t, \omega) &= \int_{-\infty}^{\infty} x^*(t - \frac{\tau}{2}) x(t + \frac{\tau}{2}) h^*(t - \frac{\tau}{2}) h(t + \frac{\tau}{2}) e^{-j\omega\tau} d\tau \\ &= \int_{-\infty}^{\infty} \phi_{xx}(t, \tau) \phi_{hh}(t, \tau) e^{-j\omega\tau} d\tau. \end{aligned} \quad (9.64)$$

The multiplication of  $\phi_{xx}(t, \tau)$  and  $\phi_{hh}(t, \tau)$  with respect to  $\tau$  can be replaced by a convolution in the frequency domain:

$$\begin{aligned} W_{\tilde{x}\tilde{x}}(t, \omega) &= \frac{1}{2\pi} W_{xx}(t, \omega) \overset{\omega}{*} W_{hh}(t, \omega) \\ &= \frac{1}{2\pi} \int_{\omega'} W_{xx}(t, \omega') W_{hh}(t, \omega - \omega') d\omega'. \end{aligned} \quad (9.65)$$

That is, a multiplication in the time domain is equivalent to a convolution of the Wigner distributions  $W_{xx}(t, \omega)$  and  $W_{hh}(t, \omega)$  with respect to  $\omega$ .

**Convolution in the Time Domain.** Convolving  $x(t)$  and  $h(t)$ , or equivalently, multiplying  $X(\omega)$  and  $H(\omega)$ , leads to a convolution of the Wigner distributions  $W_{xx}(t, \omega)$  and  $W_{hh}(t, \omega)$  with respect to  $t$ . For

$$\tilde{x}(t) = x(t) * h(t) \quad (9.66)$$

we have

$$\begin{aligned} W_{\tilde{x}\tilde{x}}(t, \omega) &= W_{xx}(t, \omega) \overset{t}{*} W_{hh}(t, \omega) \\ &= \int_{t'} W_{xx}(t', \omega) W_{hh}(t - t', \omega) dt'. \end{aligned} \quad (9.67)$$

**Pseudo-Wigner Distribution.** A practical problem one encounters when calculating the Wigner distribution of an arbitrary signal  $x(t)$  is that (9.28) can only be evaluated for a time-limited  $x(t)$ . Therefore, the concept of windowing is introduced. For this, one usually does not apply a single window

$h(t)$  to  $x(t)$ , as in (9.65), but one centers  $h(t)$  around the respective time of analysis:

$$W_{xx}^{(PW)}(t, \omega) := \int_{-\infty}^{\infty} x^*\left(t - \frac{\tau}{2}\right) x\left(t + \frac{\tau}{2}\right) h(\tau) e^{-j\omega\tau} d\tau. \quad (9.68)$$

Of course, the time-frequency distribution according to (9.68) corresponds only approximately to the Wigner distribution of the original signal. Therefore one speaks of a *pseudo-Wigner distribution* [26].

Using the notation

$$W_{xx}^{(PW)}(t, \omega) = \int_{-\infty}^{\infty} h(\tau) \phi_{xx}(t, \tau) e^{-j\omega\tau} d\tau \quad (9.69)$$

it is obvious that the pseudo-Wigner distribution can be calculated from  $W_{xx}(t, \omega)$  as

$$\begin{aligned} W_{xx}^{(PW)}(t, \omega) &= \frac{1}{2\pi} W_{xx}(t, \omega) * H(\omega) \\ &= \frac{1}{2\pi} \int_{-\infty}^{\infty} W_{xx}(t, \omega') H(\omega - \omega') d\omega' \end{aligned} \quad (9.70)$$

with  $H(\omega) \longleftrightarrow h(t)$ . This means that the pseudo-Wigner distribution is a smoothed version of the Wigner distribution.

## 9.3 General Time-Frequency Distributions

The previous section showed that the Wigner distribution is a perfect time-frequency analysis instrument as long as there is a linear relationship between instantaneous frequency and time. For general signals, the Wigner distribution takes on negative values as well and cannot be interpreted as a “true” density function. A remedy is the introduction of additional two-dimensional smoothing kernels, which guarantee for instance that the time-frequency distribution is positive for all signals. Unfortunately, depending on the smoothing kernel, other desired properties may get lost. To illustrate this, we will consider several shift-invariant and affine-invariant time-frequency distributions.

### 9.3.1 Shift-Invariant Time-Frequency Distributions

Cohen introduced a general class of time-frequency distributions of the form [29]

$$T_{xx}(t, \omega) = \frac{1}{2\pi} \iiint e^{j\nu(u-t)} g(\nu, \tau) x^*(u - \frac{\tau}{2}) x(u + \frac{\tau}{2}) e^{-j\omega\tau} d\nu du d\tau. \tag{9.71}$$

This class of distributions is also known as *Cohen's class*. Since the kernel  $g(\nu, \tau)$  in (9.71) is independent of  $t$  and  $\omega$ , all time-frequency distributions of Cohen's class are shift-invariant. That is,

$$\tilde{x}(t) = x(t - t_0) \Rightarrow T_{\tilde{x}\tilde{x}}(t, \omega) = T_{xx}(t - t_0, \omega), \tag{9.72}$$

$$\tilde{x}(t) = x(t)e^{j\omega_0 t} \Rightarrow T_{\tilde{x}\tilde{x}}(t, \omega) = T_{xx}(t, \omega - \omega_0).$$

By choosing  $g(\nu, \tau)$  all possible shift-invariant time-frequency distributions can be generated. Depending on the application, one can choose a kernel that yields the required properties.

If we carry out the integration over  $u$  in (9.71), we get

$$T_{xx}(t, \omega) = \frac{1}{2\pi} \iint g(\nu, \tau) A_{xx}(\nu, \tau) e^{-j\nu t} e^{-j\omega\tau} d\nu d\tau. \tag{9.73}$$

This means that the time-frequency distributions of Cohen's class are computed as two-dimensional Fourier transforms of two-dimensionally windowed ambiguity functions. From (9.73) we derive the Wigner distribution for  $g(\nu, \tau) = 1$ . For  $g(\nu, \tau) = h(\tau)$  we obtain the pseudo-Wigner distribution. The product

$$M(\nu, \tau) = g(\nu, \tau) A_{xx}(\nu, \tau) \tag{9.74}$$

is known as the *generalized ambiguity function*.

Multiplying  $A_{xx}(\nu, \tau)$  with  $g(\nu, \tau)$  in (9.73) can also be expressed as the convolution of  $W_{xx}(t, \omega)$  with the Fourier transform of the kernel:

$$\begin{aligned} T_{xx}(t, \omega) &= \frac{1}{2\pi} W_{xx}(t, \omega) ** G(t, \omega) \\ &= \frac{1}{2\pi} \iint W_{xx}(t', \omega') G(t - t', \omega - \omega') dt' d\omega' \end{aligned} \tag{9.75}$$

with

$$G(t, \omega) = \frac{1}{2\pi} \iint g(\nu, \tau) e^{-j\nu t} e^{-j\omega\tau} d\nu d\tau. \tag{9.76}$$

That is, all time-frequency distributions of Cohen's class can be computed by means of a convolution of the Wigner distribution with a two-dimensional impulse response  $G(t, \omega)$ .

In general the purpose of the kernel  $g(\nu, \tau)$  is to suppress the interference terms of the ambiguity function which are located far from the origin of the  $\tau$ - $\nu$  plane (see Figure 9.5); this again leads to reduced interference terms in the time-frequency distribution  $T_{xx}(t, \omega)$ . Equation (9.75) shows that the reduction of the interference terms involves "smoothing" and thus results in a reduction of time-frequency resolution.

Depending on the type of kernel, some of the desired properties of the time-frequency distribution are preserved while others get lost. For example, if one wants to preserve the characteristic

$$\frac{1}{2\pi} \int_{-\infty}^{\infty} T_{xx}(t, \omega) d\omega = |x(t)|^2, \quad (9.77)$$

the kernel must satisfy the condition

$$g(\nu, 0) = 1. \quad (9.78)$$

We realize this by substituting (9.73) into (9.77) and integrating over  $d\omega$ ,  $d\tau$ ,  $d\nu$ . Correspondingly, the kernel must satisfy the condition

$$g(0, \tau) = 1 \quad (9.79)$$

in order to preserve the property

$$\int_{-\infty}^{\infty} T_{xx}(t, \omega) dt = |X(\omega)|^2. \quad (9.80)$$

A real distribution, that is

$$T_{xx}(t, \omega) = T_{xx}^*(t, \omega), \quad (9.81)$$

is obtained if the kernel satisfies the condition

$$g(\nu, \tau) = g^*(-\nu, -\tau). \quad (9.82)$$

Finally it shall be noted that although (9.73) gives a straightforward interpretation of Cohen's class, the implementation of (9.71) is more advantageous. For this, we first integrate over  $\nu$  in (9.71). With

$$r(u, \tau) = \frac{1}{2\pi} \int_{-\infty}^{\infty} g(\nu, \tau) e^{j\nu u} d\nu \quad (9.83)$$

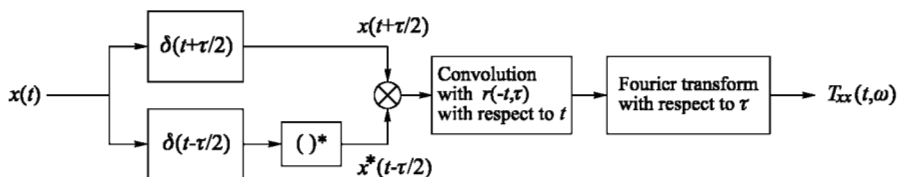


**Figure 9.6.** Generation of a general time-frequency distribution of Cohen's class.

we obtain

$$T_{xx}(t, \omega) = \iint r(u - t, \tau) x^*(u - \frac{\tau}{2}) x(u + \frac{\tau}{2}) e^{-j\omega\tau} du d\tau. \quad (9.84)$$

Figure 9.6 shows the corresponding implementation.

### 9.3.2 Examples of Shift-Invariant Time-Frequency Distributions

**Spectrogram.** The best known example of a shift-invariant time-frequency distribution is the spectrogram, described in detail in Chapter 7. An interesting relationship between the spectrogram and the Wigner distribution can be established [26]. In order to explain this, the short-time Fourier transform is expressed in the form

$$\mathcal{F}_x(t, \omega) = \int_{-\infty}^{\infty} x(t') h^*(t - t') e^{-j\omega t'} dt'. \quad (9.85)$$

Then the spectrogram is

$$S_x(t, \omega) = |\mathcal{F}_x(t, \omega)|^2 = \left| \int_{-\infty}^{\infty} x(t') h^*(t - t') e^{-j\omega t'} dt' \right|^2. \quad (9.86)$$

Alternatively, with the abbreviation

$$x_t(t') = x(t') h^*(t - t'), \quad (9.87)$$

(9.85) can be written as

$$S_{x_t}(\omega) = |X_t(\omega)|^2. \quad (9.88)$$

Furthermore, the energy density  $|X_t(\omega)|^2$  can be computed from the Wigner distribution  $W_{x_t x_t}(t', \omega)$  according to (9.31):

$$|X_t(\omega)|^2 = \int_{-\infty}^{\infty} W_{x_t x_t}(t', \omega) dt' \quad (9.89)$$

Observing (9.35) and (9.65), we finally obtain from (9.89):

$$\begin{aligned} S_x(t, \omega) &= \frac{1}{2\pi} \iint W_{xx}(t', \omega') W_{hh}(t - t', \omega - \omega') dt' d\omega' \\ &= \frac{1}{2\pi} W_{xx}(t, \omega) ** W_{hh}(t, \omega). \end{aligned} \quad (9.90)$$

Thus the spectrogram results from the convolution of  $W_{xx}(t, \omega)$  with the Wigner distribution of the impulse response  $h(t)$ . Therefore, the spectrogram belongs to Cohen's class. The kernel  $g(\nu, \tau)$  in (9.73) is the ambiguity function of the impulse response  $h(t)$  (cf. (9.75)):

$$g(\nu, \tau) = A_{hh}(\nu, \tau) = \int_{-\infty}^{\infty} h^*(t - \frac{\tau}{2}) h(t + \frac{\tau}{2}) e^{j\nu t} dt. \quad (9.91)$$

Although the spectrogram has the properties (9.81) and (9.72), the resolution in the time-frequency plane is restricted in such a way (uncertainty principle) that (9.77) and (9.80) cannot be satisfied. This becomes immediately obvious when we think of the spectrogram of a time-limited signal (see also Figure 9.2).

**Separable Smoothing Kernels.** Using separable smoothing kernels

$$g(\nu, \tau) = G_1(\nu) g_2(\tau), \quad (9.92)$$

means that smoothing along the time and frequency axis is carried out separately. This becomes obvious in (9.75), which becomes

$$\begin{aligned} T_{xx}(t, \omega) &= \frac{1}{2\pi} G(t, \omega) ** W_{xx}(t, \omega) \\ &= \frac{1}{2\pi} g_1(t) * [ G_2(\omega) * W_{xx}(t, \omega) ] \end{aligned} \quad (9.93)$$

where

$$G(t, \omega) = g_1(t) G_2(\omega), \quad g_1(t) \longleftrightarrow G_1(\omega), \quad G_2(\omega) \longleftrightarrow g_2(t). \quad (9.94)$$

From (9.83) and (9.84) we derive the following formula for the time-frequency distribution, which can be implemented efficiently:

$$T_{xx}(t, \omega) = \int \left[ \int x^*(u - \frac{\tau}{2}) x(u + \frac{\tau}{2}) g_1(u - t) du \right] g_2(\tau) e^{-j\omega\tau} d\tau. \quad (9.95)$$

Time-frequency distributions which are generated by means of a convolution of a Wigner distribution with separable impulse responses can also be understood as temporally smoothed pseudo-Wigner distributions. The window

$g_2(\tau)$  in (9.95) plays the role of  $h(\tau)$  in (9.68). Temporal smoothing is achieved by filtering with  $g_1(t)$ .

An often used smoothing kernel (especially in speech analysis) is the Gaussian

$$g(\nu, \tau) = \frac{1}{2} e^{-\alpha^2 \nu^2 / 4} e^{-\beta^2 \tau^2 / 4}, \quad \alpha, \beta \in \mathbb{R}, \alpha, \beta > 0. \quad (9.96)$$

Thus we derive the distribution

$$T_{xx}^{(\text{Gauss})}(t, \omega) = \frac{1}{2\alpha\sqrt{\pi}} \iint e^{-(u-t)^2/\alpha^2 - \frac{\beta^2}{4}\tau^2 - j\omega\tau} x^*(u - \frac{\tau}{2}) x(u + \frac{\tau}{2}) du d\tau. \quad (9.97)$$

For the two-dimensional impulse response  $G(t, \omega)$  we have

$$G(t, \omega) = g_1(t) G_2(\omega) \quad (9.98)$$

with

$$g_1(t) = \frac{1}{\alpha} e^{-t^2/\alpha^2} \quad (9.99)$$

and

$$G_2(\omega) = \frac{1}{\beta} e^{-\omega^2/\beta^2}. \quad (9.100)$$

It can be shown that for arbitrary signals a positive distribution is obtained if [75]

$$\alpha\beta \geq 1. \quad (9.101)$$

For  $\alpha\beta = 1$ ,  $T_{xx}^{(\text{Gauss})}(t, \omega)$  is equivalent to a spectrogram with Gaussian window. For  $\alpha\beta > 1$ ,  $T_{xx}^{(\text{Gauss})}(t, \omega)$  is even more smoothed than a spectrogram.

Since  $T_{xx}^{(\text{Gauss})}(t, \omega)$  for  $\alpha\beta \geq 1$  can be computed much more easily and more efficiently via a spectrogram, computing with the smoothed pseudo-Wigner distribution is interesting only for the case

$$\alpha\beta < 1. \quad (9.102)$$

The choice of  $\alpha$  and  $\beta$  is dependent on the signal in question. In order to give a hint, consider a signal  $x(t)$  consisting of the sum of two modulated time-shifted Gaussians. It is obvious that smoothing should be carried out towards the direction of the modulation of the cross term (compare Figures 9.4 and 9.5). Although the modulation may occur in any direction, we look at

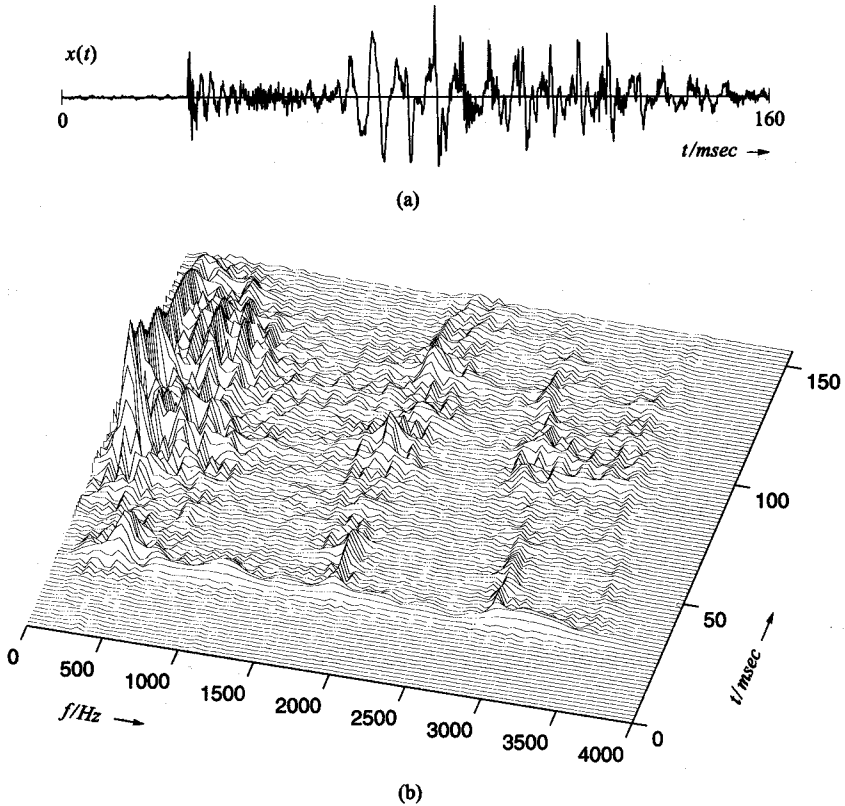


**Figure 9.7.** Time-frequency analysis of the word “taxi”. The signal and the time-frequency distribution are shown up to the beginning of the “x”; (a) time signal; (b) smoothed pseudo-Wigner distribution.

time and frequency separately. For a signal  $x(t) = x_0(t)e^{j\omega_1 t} + x_0(t)e^{j\omega_2 t}$  with  $\omega_2 > \omega_1$ , the cross-term is modulated along the time axis with frequency  $\omega_2 - \omega_1$  (compare Figure 9.4(a)). Therefore one should choose  $\alpha > 2\pi/(\omega_2 - \omega_1)$  in order to achieve efficient smoothing. The superposition of two signal components which are identical except for a time shift  $x(t) = x_0(t - t_1) + x_0(t - t_2)$ , leads to a cross-term that is modulated along the frequency axis (compare Figure 9.4(b)). Here,  $\beta$  must be chosen just large enough to achieve efficient smoothing of the oscillations along the frequency axis.

Figure 9.7 shows the smoothed pseudo-Wigner distribution of a speech signal, and Figure 9.8 shows two corresponding spectrograms. The time resolution in Figure 9.7 is the same as in Figure 9.8(a), while the frequency resolution in Figure 9.7 is the same as in Figure 9.8(b).

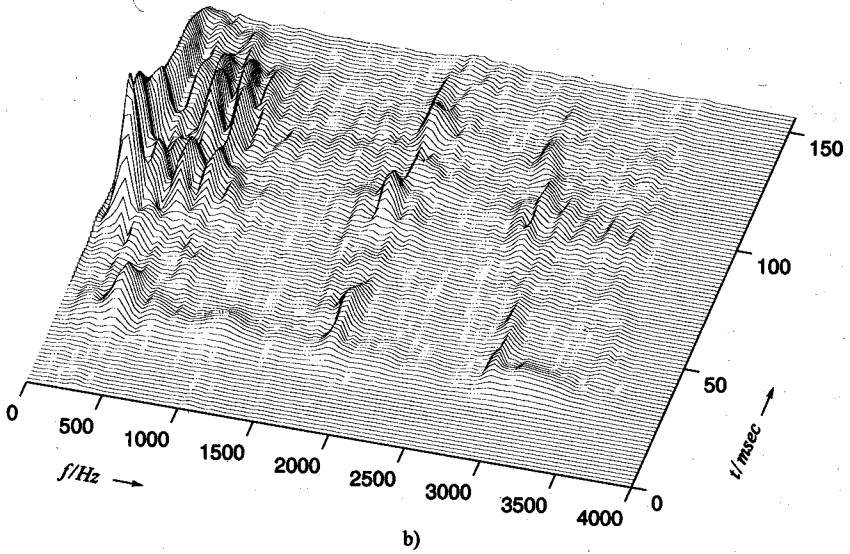
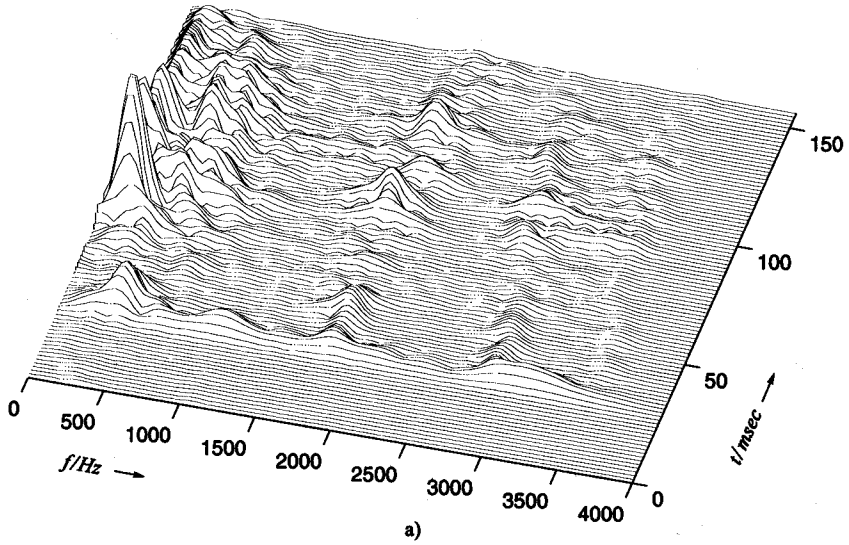


**Figure 9.8.** Spectrogram of the signal shown in Figure 9.7; (a) good time resolution; (b) good frequency resolution.

**Examples of Time-Frequency Distributions of Cohen's Class.** In the literature we find many proposals of shift-invariant time-frequency distributions. A survey is presented in [72] for instance. In the following, three examples will briefly be mentioned.

*Rihaczek distribution.* The Rihaczek distribution is defined as [124]

$$\begin{aligned} T_{xx}^{(R)}(t, \omega) &= \int x^*(t) x(t + \tau) e^{-j\omega\tau} d\tau \\ &= x^*(t) X(\omega) e^{j\omega t}. \end{aligned} \quad (9.103)$$

This type of distribution is of enticing simplicity, but it is not real-valued in general.

*Choi-Williams Distribution.* For the Choi-Williams distribution the following product kernel is used [24]:

$$g(\nu, \tau) = e^{-\nu^2 \tau^2 / (4\pi^2 \sigma)}, \quad \sigma > 0. \quad (9.104)$$

We see that  $g(\nu, 0) = 1$  and  $g(0, \tau) = 1$  are satisfied so that the Choi-Williams distribution has the properties (9.77) and (9.80).

The quantity  $\sigma$  in (9.104) may be understood as a free parameter. If a small  $\sigma$  is chosen, the kernel concentrates around the origin of the  $\tau$ - $\nu$  plane, except for the  $\tau$  and the  $\nu$  axis. Thus we get a generalized ambiguity function  $M(\nu, \tau) = g(\nu, \tau) A_{xx}(\nu, \tau)$  with reduced interference terms, and the corresponding time-frequency distribution has reduced interference terms as well. From (9.71), (9.83), and (9.84) we get

$$T_{xx}^{(CW)}(t, \omega) = \int_{-\infty}^{\infty} \int_{-\infty}^{\infty} \sqrt{\frac{\pi\sigma}{\tau^2}} e^{-\pi^2 \sigma (u-t)^2 / \tau^2} x^*(u - \frac{\tau}{2}) x(u + \frac{\tau}{2}) e^{-j\omega\tau} du d\tau. \quad (9.105)$$

*Zhao-Atlas-Marks Distribution.* Zhao, Atlas and Marks [168] suggested the kernel

$$g(\nu, \tau) = g_1(\tau) \frac{2 \sin(\nu|\tau|/a)}{\nu}. \quad (9.106)$$

This yields the distribution

$$T_{xx}^{(ZAM)}(t, \omega) = \int_{-\infty}^{\infty} g_1(\tau) e^{-j\omega\tau} \int_{t-|\tau|/a}^{t+|\tau|/a} x^*(u - \frac{\tau}{2}) x(u + \frac{\tau}{2}) du d\tau. \quad (9.107)$$

### 9.3.3 Affine-Invariant Time-Frequency Distributions

Affine smoothing is an alternative to regular smoothing of the Wigner distribution (Cohen’s class). A time-frequency distribution that belongs to the affine class is invariant with respect to time shift and scaling:

$$\tilde{x}(t) = \sqrt{|a|} x(a(t - t_0)) \quad \Rightarrow \quad T_{\tilde{x}\tilde{x}}(t, \omega) = T_{xx}(a(t - t_0), \omega/a). \quad (9.108)$$

Any time-frequency distribution that satisfies (9.108) can be computed from the Wigner distribution by means of an affine transform [54], [126]:

$$T_{xx}(t, \omega) = \frac{1}{2\pi} \iint K(\omega(t' - t), \omega'/\omega) W_{xx}(t', \omega') dt' d\omega'. \quad (9.109)$$

This can be understood as correlating the Wigner distribution with kernel  $K$  along the time axis. By varying  $\omega$  the kernel is scaled.

Since (9.108) and (9.72) do not exclude each other, there exist other time-frequency distributions besides the Wigner distribution which belong to the shift-invariant Cohen class as well as to the affine class. These are, for instance, all time-frequency distributions that originate from a product kernel, such as the Choi–Williams distribution.

**Scalogram.** An example of the affine class is the scalogram, that is, the squared magnitude of the wavelet transform of a signal:

$$|\mathcal{W}_x(b, a)|^2 = \left| \int_{-\infty}^{\infty} x(t) \psi_{b,a}^*(t) dt \right|^2 \quad (9.110)$$

with

$$\psi_{b,a}(t) = |a|^{-\frac{1}{2}} \psi\left(\frac{t-b}{a}\right). \quad (9.111)$$

Moyal’s formula (9.42) yields the relationship

$$|\mathcal{W}_x(b, a)|^2 = \frac{1}{2\pi} \iint W_{\psi_{b,a}, \psi_{b,a}}(t', \omega') W_{xx}(t', \omega') dt' d\omega', \quad (9.112)$$

where

$$W_{\psi_{b,a}, \psi_{b,a}}(t', \omega') = W_{\psi, \psi}\left(\frac{t' - b}{a}, a\omega'\right). \quad (9.113)$$

Thus, from (9.112) we derive

$$|\mathcal{W}_x(b, a)|^2 = \frac{1}{2\pi} \iint W_{\psi, \psi}\left(\frac{t' - b}{a}, a\omega'\right) W_{xx}(t', \omega') dt' d\omega'. \quad (9.114)$$

The substitutions  $b = t$  and  $a = \omega_0/\omega$  finally yield

$$\begin{aligned} T_{xx}(t, \omega) &= |\mathcal{W}_x(t, \omega_0/\omega)|^2 \\ &= \frac{1}{2\pi} \iint \mathcal{W}_{\psi, \psi} \left( \frac{\omega}{\omega_0}(t' - t), \frac{\omega_0}{\omega}\omega' \right) W_{xx}(t', \omega') dt' d\omega'. \end{aligned} \quad (9.115)$$

The resolution of the scalogram is, just like that of the spectrogram, limited by the uncertainty principle.

### 9.3.4 Discrete-Time Calculation of Time-Frequency Distributions

If we wish to calculate the Wigner distribution or some other time-frequency distribution on a computer we are forced to sample our signal and the transform kernel and to replace all integrals by sums. If the signal and the kernel are bandlimited and if the sampling rate is far above the Nyquist rate for both signal and kernel, we do not face a substantial problem. However, in some cases, such as the Choi-Williams distribution, sampling the kernel already poses a problem. On the other hand, the test signal may be discrete-time right away, so that discrete-time definitions of time-frequency distributions are required in any case.

**Discrete-Time Wigner Distribution [26].** The *discrete-time Wigner distribution* is defined as

$$W_{xx}(n, e^{j\omega}) = 2 \sum_m x^*(n - m) x(n + m) e^{-j2\omega m}. \quad (9.116)$$

Here, equation (9.116) is the discrete version of equation (9.28), which, using the substitution  $\tau' = \tau/2$ , can be written as

$$W_{xx}(t, \omega) = 2 \int_{-\infty}^{\infty} x^*(t - \tau') x(t + \tau') e^{-j2\omega\tau'} d\tau'. \quad (9.117)$$

As we know, discrete-time signals have a periodic spectrum, so that one could expect the Wigner distribution of a discrete-time signal to have a periodic spectrum also. We have the following property: while the signal  $x(n)$  has a spectrum  $X(e^{j\omega}) \leftrightarrow x(n)$  with period  $2\pi$ , the period of the discrete-time Wigner distribution is only  $\pi$ . Thus,

$$W_{xx}(n, e^{j\omega}) = W_{xx}(n, e^{j\omega + k\pi}), \quad k \in \mathbb{Z}. \quad (9.118)$$

The reason for this is subsampling by the factor two with respect to  $\tau$ . In order to avoid aliasing effects in the Wigner distribution, one has to take care that the bandlimited signal  $x(t)$  is sampled with the rate

$$f_a \geq 4 f_{max} \tag{9.119}$$

and not with  $f_a \geq 2 f_{max}$ , where

$$X(\omega) = 0 \quad \text{for } |\omega| > 2\pi f_{max}. \tag{9.120}$$

Because of the different periodicity of  $X(e^{j\omega})$  and  $W_{xx}(n, e^{j\omega})$  it is not possible to transfer all properties of the continuous-time Wigner distribution to the discrete-time Wigner distribution. A detailed discussion of the topic can be found in [26], Part II.

**General Discrete-Time Time-Frequency Distributions.** Analogous to (9.84) and (9.116), a general discrete-time time-frequency distribution of Cohen’s class is defined as

$$T_{xx}(n, k) = 2 \sum_{m=-M}^M \sum_{\ell=-N}^N \rho(\ell, m) x^*(\ell + n - m) x(\ell + n + m) e^{-j4\pi km/L}. \tag{9.121}$$

Here we have already taken into account that in practical applications one would only consider discrete frequencies  $2\pi k/L$ , where  $L$  is the DFT length.

Basically we could imagine the term  $\rho(\ell, m)$  in (9.121) to be a  $2M + 1 \times 2N + 1$  matrix which contains sample values of the function  $r(u, \tau)$  in (9.84). However, for kernels that are not bandlimited, sampling causes a problem. For example, for the discrete-time Choi–Williams distribution we therefore use the matrix

$$\rho^{(CW)}(n, m) = \begin{cases} \frac{1}{|m|} \alpha_m e^{-\sigma n^2/4m^2}, & m \neq 0, \\ \delta(n), & m = 0, \end{cases} \tag{9.122}$$

with

$$\alpha_m = \sum_{k=-N}^N \frac{1}{|m|} e^{-\sigma k^2/4m^2}, \quad n = -N, \dots, N, \quad m = -M, \dots, M. \tag{9.123}$$

The normalization  $\sum_n \rho(n, m) = 1$  in (9.122) is necessary in order to preserve the properties [11]

$$\sum_n T_{xx}^{(CW)}(n, k) = |X(k)|^2 = |X(e^{j\omega_k})|^2 \tag{9.124}$$

and

$$\sum_k T_{xx}^{(CW)}(n, k) = |x(n)|^2. \quad (9.125)$$

## 9.4 The Wigner–Ville Spectrum

So far the signals analyzed have been regarded as deterministic. Contrary to the previous considerations,  $x(t)$  is henceforth defined as a stochastic process. We may view the deterministic analyses considered so far as referring to single sample functions of a stochastic process. In order to gain information on the stochastic process we define the so-called *Wigner–Ville spectrum* as the expected value of the Wigner distribution:

$$\bar{W}_{xx}(t, \omega) = E \{W_{xx}(t, \omega)\} = \int_{-\infty}^{\infty} r_{xx}(t + \frac{\tau}{2}, t - \frac{\tau}{2}) e^{-j\omega\tau} d\tau \quad (9.126)$$

with

$$r_{xx}(t + \frac{\tau}{2}, t - \frac{\tau}{2}) = E \{\phi_{xx}(t, \tau)\} = E \left\{ x^*(t - \frac{\tau}{2}) x(t + \frac{\tau}{2}) \right\}. \quad (9.127)$$

This means that the temporal correlation function  $\phi_{xx}(t, \tau)$  is replaced by its expected value, which is the autocorrelation function  $r_{xx}(t + \frac{\tau}{2}, t - \frac{\tau}{2})$  of the process  $x(t)$ .

The properties of the Wigner–Ville spectrum are basically the same as those of the Wigner distribution. But by forming the expected value it generally contains fewer negative values than the Wigner distribution of a single sample function.

The Wigner–Ville spectrum is of special interest when analyzing non-stationary or cyclo-stationary processes because here the usual terms, such as power spectral density, do not give any information on the temporal distribution of power or energy. In order to illustrate this, the Wigner–Ville spectrum will be discussed for various processes in connection with the standard characterizations.

**Stationary Processes.** For stationary processes the autocorrelation function only depends on  $\tau$ , and the Wigner–Ville spectrum becomes the power spectral density:

$$\bar{W}_{xx}(t, \omega) = S_{xx}(\omega) = \int_{-\infty}^{\infty} r_{xx}(\tau) e^{-j\omega\tau} d\tau \quad (9.128)$$

if  $x(t)$  is stationary.

**Processes with Finite Energy.** If we assume that the process  $x(t)$  has finite energy, an average energy density spectrum can be derived from the Wigner–Ville spectrum as

$$\bar{s}_{xx}(t) = E \{|x(t)|^2\} = \frac{1}{2\pi} \int_{-\infty}^{\infty} \bar{W}_{xx}(t, \omega) d\omega, \quad (9.129)$$

$$\bar{S}_{xx}(\omega) = E \{|X(\omega)|^2\} = \int_{-\infty}^{\infty} \bar{W}_{xx}(t, \omega) dt. \quad (9.130)$$

For the mean energy we then have

$$E_x = E \left\{ \int_{-\infty}^{\infty} |x(t)|^2 dt \right\} = \frac{1}{2\pi} \int_{-\infty}^{\infty} \bar{W}_{xx}(t, \omega) d\omega dt. \quad (9.131)$$

**Non-Stationary Processes with Infinite Energy.** For non-stationary processes with infinite energy the power spectral density is not defined. However, a mean power density is given by

$$\bar{S}_{xx}(\omega) = \lim_{T \rightarrow \infty} \frac{1}{T} \int_{-T/2}^{T/2} \bar{W}_{xx}(t, \omega) dt. \quad (9.132)$$

**Cyclo-Stationary Processes.** For cyclo-stationary processes it is sufficient to integrate over one period  $T$  in order to derive the mean power density:

$$\bar{S}_{xx}(\omega) = \frac{1}{T} \int_{-T/2}^{T/2} \bar{W}_{xx}(t, \omega) dt. \quad (9.133)$$

**Example.** As a simple example of a cyclo-stationary process, we consider the signal

$$x(t) = \sum_{i=-\infty}^{\infty} d(i) g(t - iT). \quad (9.134)$$

Here,  $g(t)$  is the impulse response of a filter that is excited with statistically independent data  $d(i)$ ,  $i \in \mathbb{Z}$ . The process  $d(i)$  is assumed to be zero-mean and stationary. The signal  $x(t)$  can be viewed as the complex envelope of a real bandpass signal.

Now we consider the autocorrelation function of the process  $x(t)$ . We

obtain

$$\begin{aligned}
 r_{xx}(t + \tau, t) &= E \{x^*(t)x(t + \tau)\} \\
 &= \sum_{i=-\infty}^{\infty} \sum_{j=-\infty}^{\infty} E \{d^*(i)d(j)\} g^*(t - iT) g(t - jT + \tau) \\
 &= \sigma_d^2 \sum_{i=-\infty}^{\infty} g^*(t - iT) g(t - iT + \tau).
 \end{aligned} \tag{9.135}$$

As (9.135) shows, the autocorrelation function depends on  $t$  and  $\tau$ , and in general the process  $x(t)$  is not stationary. Nevertheless, it is cyclo-stationary, because the statistical properties repeat periodically:

$$r_{xx}(t + \tau, t) = r_{xx}(t + \tau + \ell T, t + \ell T), \quad \ell \in \mathbf{Z}. \tag{9.136}$$

Typically, one chooses the filter  $g(t)$  such that its autocorrelation function  $r_{gg}^E(\tau)$  satisfies the first Nyquist condition:

$$r_{gg}^E(mT) = \begin{cases} 1 & \text{for } m = 0, \\ 0 & \text{otherwise.} \end{cases} \tag{9.137}$$

Commonly used filters are the so-called *raised cosine filters*, which are designed as follows. For the energy density  $S_{gg}^E(\omega) \longleftrightarrow r_{gg}^E(t)$  we take

$$S_{gg}^E(\omega) = \begin{cases} 1 & \text{for } |\omega T|/\pi \leq 1 - r, \\ \frac{1}{2}[1 + \cos[\frac{\pi}{2r}(\omega T/\pi - (1 - r))]] & \text{for } 1 - r \leq |\omega T|/\pi \leq 1 + r, \\ 0 & \text{for } |\omega T|/\pi \geq 1 + r. \end{cases} \tag{9.138}$$

Here,  $r$  is known as the *roll-off factor*, which can be chosen in the region  $0 \leq r \leq 1$ . For  $r = 0$  we get the ideal lowpass. For  $r > 0$  the energy density decreases in cosine form.

From (9.138) we derive

$$r_{gg}^E(t) = \frac{1}{T} \frac{\sin \pi t/T}{\pi t/T} \frac{\cos r\pi t/T}{1 - (2rt/T)^2}. \tag{9.139}$$

As we see, for  $r > 0$ ,  $r_{gg}^E(t)$  is a windowed version of the impulse response of the ideal lowpass. Because of the equidistant zeros of the si-function, condition (9.137) is satisfied for arbitrary roll-off factors.

With

$$G(\omega) = \sqrt{S_{gg}^E(\omega)}, \tag{9.140}$$

the required impulse response  $g(t)$  can be derived from (9.138) by means of an inverse Fourier transform:

$$g(t) = \frac{(4rt/T) \cos(\pi t(1+r)/T) + \sin(\pi t(1-r)/T)}{\pi t [1 - (4rt/T)^2]} \tag{9.141}$$

where

$$\begin{aligned} g(0) &= \frac{1}{T} \left( 1 + r \left( \frac{4}{\pi} - 1 \right) \right), \\ g\left(\pm \frac{T}{4r}\right) &= -\frac{r}{T} \left[ \frac{2}{\pi} \cos\left(\frac{\pi(1+r)}{4r}\right) - \cos\left(\frac{\pi(1-r)}{4r}\right) \right]. \end{aligned} \tag{9.142}$$

Figure 9.9 shows three examples of autocorrelation functions with period  $T$  and the corresponding Wigner–Ville spectra. We observe that for large roll-off factors there are considerable fluctuations in power in the course of a period. When stating the mean power density in the classical way according to (9.133) these effects are not visible (cf. Figure 9.10).

As can be seen in Figure 9.9, the fluctuations of power decrease with vanishing roll-off factor. In the limit, the ideal lowpass is approached ( $r = 0$ ), and the process  $x(t)$  becomes wide-sense stationary. In order to show this, the autocorrelation function  $r_{xx}(t + \tau, t)$  is written as the inverse Fourier transform of a convolution of  $G^*(-\omega)$  and  $G(\omega)$ :

$$\begin{aligned} r_{xx}(t + \tau, t) &= \sigma_d^2 \sum_{k=-\infty}^{\infty} \frac{1}{4\pi^2} \int_{-\infty}^{\infty} \int_{-\infty}^{\infty} G^*(-\omega') G(\omega - \omega') \\ &\quad e^{j(\omega - \omega')\tau - j\omega kT} d\omega' e^{j\omega t} d\omega. \end{aligned} \tag{9.143}$$

Here the summation is to be performed over the complex exponentials only. Thus, by using

$$\sum_{k=-\infty}^{\infty} e^{-j\omega kT} = \frac{2\pi}{T} \sum_{k=-\infty}^{\infty} \delta\left(\omega - k \frac{2\pi}{T}\right), \tag{9.144}$$

we achieve

$$\begin{aligned} r_{xx}(t + \tau, t) &= \frac{\sigma_d^2}{2\pi T} \int_{-\infty}^{\infty} \int_{-\infty}^{\infty} G^*(-\omega') G(\omega - \omega') e^{-j\omega'\tau} \\ &\quad e^{j\omega\tau} e^{j\omega t} \sum_{k=-\infty}^{\infty} \delta\left(\omega - k \frac{2\pi}{T}\right) d\omega d\omega'. \end{aligned} \tag{9.145}$$

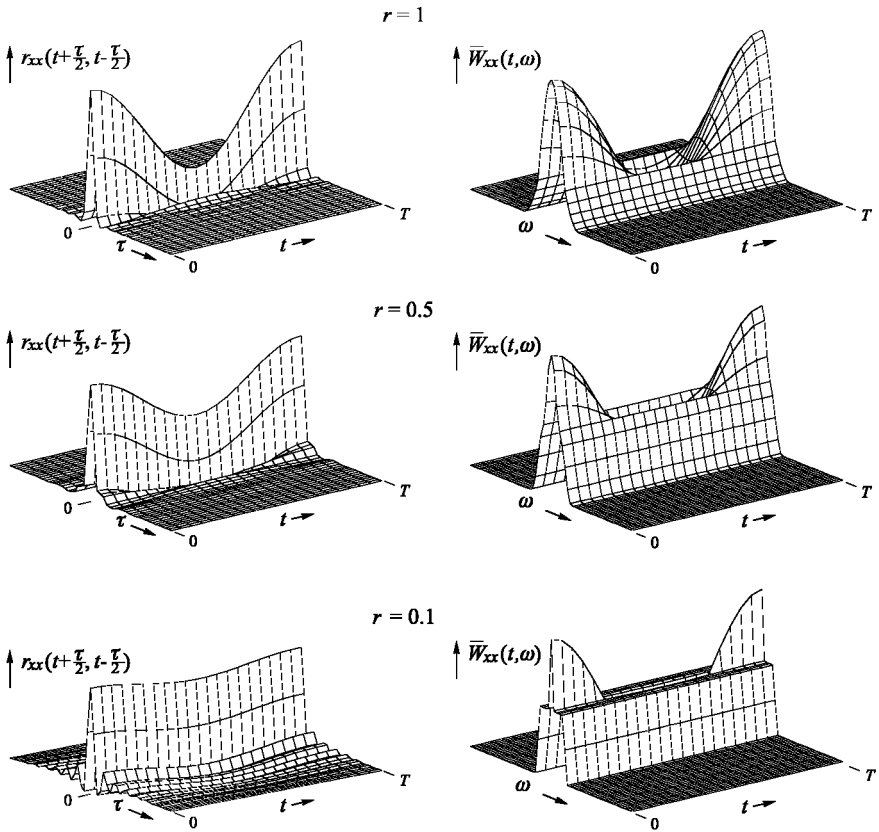


**Figure 9.9.** Periodic autocorrelation functions and Wigner-Ville spectra (raised cosine filter design with various roll-off factors  $r$ ).

Integrating over  $\omega$  yields

$$r_{xx}(t + \tau, t) = \frac{\sigma_d^2}{2\pi T} \int_{-\infty}^{\infty} \sum_{k=-\infty}^{\infty} G^*(-\omega') G(k\frac{2\pi}{T} - \omega') e^{-j\omega'\tau} e^{jk\frac{2\pi}{T}\tau} e^{jk\frac{2\pi}{T}t} d\omega'. \tag{9.146}$$

If  $G(\omega)$  is bandlimited to  $\pi/T$ , only the term for  $k = 0$  remains, and the

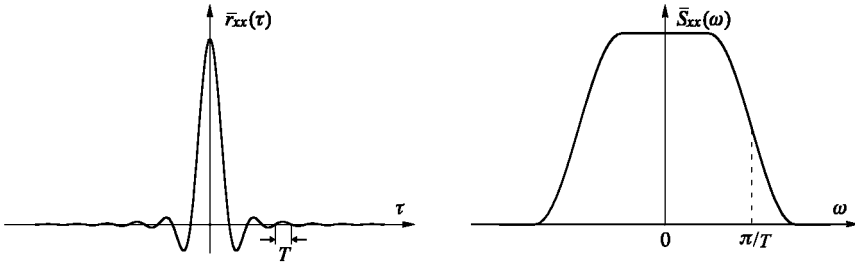


**Figure 9.10.** Mean autocorrelation functions  $\bar{r}_{xx}(\tau) = \frac{1}{T} \int_0^T r_{x'x'}(t + \tau, t) dt$  and mean power spectral density ( $r = 0.5$ ).

autocorrelation function depends on  $\tau$  only:

$$\begin{aligned}
 r_{xx}(t + \tau, t) &= \sigma_d^2 \frac{1}{2\pi T} \int_{-\infty}^{\infty} G^*(-\omega') G(-\omega') e^{-j\omega'\tau} d\omega' \\
 &= \sigma_d^2 \frac{1}{2\pi T} \int_{-\infty}^{\infty} S_{gg}^E(\omega') e^{j\omega'\tau} d\omega' \tag{9.147} \\
 &= \sigma_d^2 \frac{1}{T} r_{gg}^E(\tau).
 \end{aligned}$$

This shows that choosing  $g(t)$  to be the ideal lowpass with bandwidth  $\pi/T$  yields a Nyquist system in which  $x(t)$  is a wide-sense stationary process. However, if we consider realizable systems we must assume a cyclo-stationary process.

Stationarity within a realizable framework can be obtained by introducing a delay of half a sampling period for the imaginary part of the signal. An example of such a modulation scheme is the well-known offset phase shift keying. The modified signal reads

$$x'(t) = \sum_{i=-\infty}^{\infty} \Re\{d(i)\} g(t - iT) + j\Im\{d(i)\} g(t - iT - T/2). \tag{9.148}$$

Assuming that

$$\begin{aligned}
 E \{ \Re\{d(i)\} \Re\{d(j)\} \} &= \frac{1}{2} \sigma_d^2 \delta_{ij}, \\
 E \{ \Im\{d(i)\} \Im\{d(j)\} \} &= \frac{1}{2} \sigma_d^2 \delta_{ij}, \tag{9.149} \\
 E \{ \Re\{d(i)\} \Im\{d(j)\} \} &= 0, \quad i, j \in \mathbf{Z},
 \end{aligned}$$

we have

$$\begin{aligned}
 r_{x'x'}(t + \tau, t) &= \frac{1}{2}\sigma_d^2 \sum_{i=-\infty}^{\infty} g^*(t - iT) g(t - iT + \tau) \\
 &+ \frac{1}{2}\sigma_d^2 \sum_{i=-\infty}^{\infty} g^*(t - iT - \frac{T}{2}) g(t - iT + \tau - \frac{T}{2}) \\
 &= \frac{1}{2}\sigma_d^2 \sum_{i=-\infty}^{\infty} g^*(t - i\frac{T}{2}) g(t + \tau - i\frac{T}{2})
 \end{aligned} \tag{9.150}$$

for the autocorrelation function. According to (9.146) this can be written as

$$\begin{aligned}
 r_{x'x'}(t + \tau, t) &= \\
 &\frac{\sigma_d^2}{2\pi T} \int_{-\infty}^{\infty} \sum_{k=-\infty}^{\infty} G^*(-\omega') G(k\frac{4\pi}{T} - \omega') e^{-j\omega'\tau} e^{jk\frac{4\pi}{T}\tau} e^{jk\frac{4\pi}{T}t} d\omega'.
 \end{aligned} \tag{9.151}$$

We see that only the term for  $k = 0$  remains if  $G(\omega)$  is bandlimited to  $2\pi/T$ , which is the case for the raised cosine filters. The autocorrelation function then is

$$r_{x'x'}(t + \tau, t) = \sigma_d^2 \frac{1}{T} r_{gg}^E(\tau). \tag{9.152}$$

Hence the autocorrelation function  $r_{x'x'}(t + \tau, t)$  and the mean autocorrelation function are identical. Correspondingly, the Wigner–Ville spectrum equals the mean power spectral density.

If we regard  $x'(t)$  as the complex envelope of a real bandpass process  $x_{\text{BP}}(t)$ , then we cannot conclude from the wide-sense stationarity of  $x'(t)$  the stationarity of  $x_{\text{BP}}(t)$ : for this to be true, the autocorrelation functions  $r_{x_R x_R}(t + \tau, t)$  and  $r_{x_I x_I}(t + \tau, t)$  would have to be identical and would have to be dependent only on  $\tau$  (cf. Section 2.5).